

Lump scattering on the torus

RJ Cova*

Departamento de Física F.E.C.

La Universidad del Zulia

Apartado 15332

Maracaibo 4005-A

Venezuela

February 2000

Abstract

Head-on collisions between two solitons in the pure CP^1 model on a flat torus are investigated via numerical simulations. The charge-two lumps, written out in terms of Weierstrass' elliptic \wp -function, are found to scatter at 90° . The phenomenon of singularity formation is also seen.

1 Introduction

The non-linear $O(3)$ sigma or CP^1 model in three-dimensional space-time is a rich industry of research, both for its condensed matter applications and as a simple field theory possessing topological solitons. The energy density associated with the solitons are lumps localised in space. The model also appears as a low dimensional analogue of non-abelian gauge field theories in (3+1) dimensions, an example being the increasingly popular Skyrme model of nuclear physics. In pure mathematics the CP^1 solitons are known as harmonic maps, by itself a long established area of research.

The classical (2+0)-dimensional CP^1 model on the extended plane or Riemann sphere $\mathfrak{R}_2 \cup \{\infty\} \simeq S_2$, where the solitons are harmonic maps $S_2 \mapsto S_2$ given by any complex holomorphic function, has been amply discussed in the literature [1, 2]. The full time-dependent model [(2+1) dimensions] is not integrable, so numerical simulations are needed for studying its dynamics. Regarding collisions, it is well known that the lumps on the extended plane scatter-off at 90° with respect to the initial direction of motion in the centre-of-mass frame [3]. Due to the conformal invariance of the planar model, the lumps are unstable in the sense that they can shrink indefinitely, leading to singularity formation in finite time [4]. This instability is cured by supplementing the $O(3)$ lagrangian with a Skyrme-like and a potential-like term [5].

More recently, attention has also been paid to the CP^1 model with square periodic boundary conditions, where the solitons are harmonic maps $T_2 \mapsto S_2$ (T_2 a flat torus) given by elliptic functions. Physically, this approach looks more attractive than the one on S_2 because the system is located in a finite volume from the outset. Mathematically, the model on T_2 has the formal advantage of removing the problem confronted in the extended plane, whose non-compactness brings about difficulties to defining the metric on the moduli space of static soliton solutions.

In reference [6] we tackled the toroidal model by expressing the soliton fields in terms of Weierstrass' σ -function. We found several properties not seen in the usual planar theory, principally that there are no single-soliton solutions on the torus and, in the Skyrme version of the model, that there is no critical speed below which the skyrmions do not scatter at 90° .

*rcova@luz.ve

Our anterior paper [7] resorted to the Weierstrass' elliptic \wp -function to numerically study the CP^1 model, both in its original and Skyrme versions, for systems with no initial speed. Novel features were unveiled in the topological charge two sector. Amongst them: • the appearance of four energy chunks instead of two for certain configurations initially situated in the diagonals of the lattice and • lump splitting in the Skyrme case for systems initially located in the central cross of the grid.

Within the framework of the geodesic approximation, the elliptic \wp -function was employed as well by Speight [8] to describe pure CP^1 lumps. His analysis predicted that the solitons may shrink and form singularities in finite time –as their siblings on S_2 – and that the solitons should also scatter at 90° .

In the present paper we report the results for CP^1 lump scattering obtained by numerically simulating the initial-value problem given by the Weierstrass' \wp -function in the original, unmodified CP^1 model. Our results bear out the predictions referred to in the previous paragraph.

The paper is arranged as follows: In the next section we lay out the CP^1 model with periodic boundary conditions. In section 3 the numerical procedure is explained and in section 4 the scattering results are discussed. We close the paper with some concluding remarks including suggestions for further research.

2 The CP^1 model on the torus

Our model is defined by the lagrangian density

$$\mathcal{L} = \frac{|\partial_t W|^2 - 2|\partial_z W|^2 - 2|\partial_{\bar{z}} W|^2}{(1 + |W|^2)^2} \quad (1)$$

where $z = x + iy \in T_2$; \bar{z} is the complex conjugate of z . The complex field W obeys the periodic boundary condition

$$W[z + (m + in)L] = W(z), \quad \forall t, \quad (2)$$

where $m, n = 0, 1, 2, \dots$ and L is the size of the torus. The static soliton solutions are elliptic functions which may be written as

$$W = \lambda \wp(z - a) + b, \quad \lambda, a, b \in \mathcal{Z}, \quad (3)$$

being $\wp(z)$ the elliptic function of Weierstrass. Within a *fundamental cell* of vertices

$$(0, 0), (L, 0), (L, L), (0, L),$$

\wp is expandable as [9]

$$\wp(z) = z^{-2} + \xi_2 z^2 + \xi_3 z^4 + \dots + \xi_j z^{2j-2} + \dots, \quad \xi_j \in \mathfrak{R}. \quad (4)$$

This function is of the second order (degree) and so (3) represents solitons of topological charge 2. As discussed in [6, 7] a distinctive feature of the toroidal model is the absence of analytical single-soliton solutions. This can be understood by recalling that the simplest non-trivial elliptic function is of order 2. In the language of differential geometry, the degree of the harmonic maps $M \mapsto S_2$ must be greater than $genus(M)$, M a compact and orientable Riemann surface. Since $genus(T_2) = 1$ there are no unit-degree maps on the torus. However, a periodic single-soliton *ansatz* was constructed in [6] using the equation (5) below with $\kappa=1$ and relaxing the accompanying selection rule. Note that when $M = S_2$ we have the common model with standard boundary conditions which do possess solitons in all homotopy classes; this is because $genus(S_2) = 0$.

In reference [6] we computed the periodic solitons through

$$W = \prod_{j=1}^{\kappa} \frac{\sigma(z - a_j)}{\sigma(z - b_j)}, \quad \sum_{j=1}^{\kappa} a_j = \sum_{j=1}^{\kappa} b_j, \quad (5)$$

with a subroutine that calculates $\sigma(z)$ numerically. Although σ is pseudo-elliptic, the above ratio subject to the summation of its zeros (a_j) being equal to the summation of its poles (b_j) renders W elliptic. In this paper we utilise a similar subroutine and then reckon $\wp(z)$ using the formula [9]:

$$\wp(z) = -\frac{d^2}{dz^2} \ln[\sigma(z)]. \quad (6)$$

The Laurent expansion for σ reads

$$\sigma(z) = \sum_{j=0}^{\infty} c_j z^{4j+1}, \quad c_j \in \mathfrak{R}. \quad (7)$$

Assisted by the useful properties of $\wp(z)$:

$$\wp(z) = \wp(-z), \quad \wp(iz) = -\wp(z), \quad \wp(\bar{z}) = \overline{\wp(z)}, \quad (8)$$

one readily deduces that $\wp(z)$ is real on the boundary and central cross of the fundamental cell, and purely imaginary on the borders [10].

The *static* (or potential) energy density E associated with the harmonic map W may be read-off from the lagrangian (1). Taking into account the identity [10]

$$\left[\frac{d\wp(z-a)}{dz}\right]^2 = 4\wp(z-a)[\wp(z-a)^2 - \wp^2(L/2)], \quad (9)$$

we have

$$E = 8|\lambda|^2 \frac{|\wp(z-a)|[\wp^2(z-a) - \wp^2(L/2)]}{[1 + |\lambda\wp(z-a) + b|^2]}. \quad (10)$$

3 Basic numerical procedure

We treat configurations of the form (3) as the initial conditions for our time evolution, studied numerically. The time derivative of W is calculated from the Lorentz-boosted field. Our simulations run in the ϕ -formulation of the model, whose field equation

$$\partial_t^2 \vec{\phi} = [-(\partial_t \vec{\phi})^2 + (\partial_x \vec{\phi})^2 + (\partial_y \vec{\phi})^2] \vec{\phi} + \partial_x^2 \vec{\phi} + \partial_y^2 \vec{\phi} \quad (11)$$

follows from the lagrangian density (1) with the help of

$$W = \frac{1 - \phi_3}{\phi_1 + i\phi_2}. \quad (12)$$

The real scalar field $\vec{\phi} = (\phi_1, \phi_2, \phi_3)$ satisfies $\vec{\phi} \cdot \vec{\phi} = 1$. Inverting formula (12) entails

$$\vec{\phi} = \left(\frac{W + \bar{W}}{|W|^2 + 1}, i \frac{-W + \bar{W}}{|W|^2 + 1}, \frac{|W|^2 - 1}{|W|^2 + 1} \right). \quad (13)$$

We compute the series (7) up to the fifth term, the coefficients c_j being in our case negligibly small for $j \geq 6$. We employ the fourth-order Runge-Kutta method and approximate the spatial derivatives by finite differences. The laplacian is evaluated using the standard nine-point formula and, to further check our results, a 13-point recipe is also used. Our results show unsensitiveness to either technique, thus confirming the reliability of our results. The discrete model evolves on a 200×200 periodic lattice ($n_x = n_y = 200$) with spatial and time steps $\delta x = \delta y = 0.02$ and $\delta t = 0.005$, respectively. The size of our fundamental, toroidal network is $L = n_x \times \delta x = 4$.

Unavoidable round-off errors gradually shift the fields away from the constraint $\vec{\phi} \cdot \vec{\phi} = 1$. So we rescale $\vec{\phi} \rightarrow \vec{\phi} / \sqrt{\vec{\phi} \cdot \vec{\phi}}$ every few iterations. Each time, just before the rescaling operation, we evaluate the quantity $\mu \equiv \vec{\phi} \cdot \vec{\phi} - 1$ at each lattice point. Treating the maximum of the absolute value of μ as a measure of the numerical errors, we find that $\max|\mu| \approx 10^{-10}$. This magnitude is useful as a guide to determine how reliable a given numerical result is. Usage of an unsound numerical procedure in the Runge-Kutta evolution shows itself as a rapid growth of $\max|\mu|$; this also occurs, for instance, when the unstable energy lumps become too spiky.

4 Results

The initial conditions are then given by equation (3)

$$W = \lambda \wp(z - a) + b,$$

where λ is related to the size of the solitons, b determines their mutual separation and a merely shifts the solution on the torus. Calling the initial speed v , we boost the above field and take its time derivative:

$$\begin{aligned} W \rightarrow W(t) &= \lambda \wp(z - a) + b(1 - vt), \\ \partial_t W(t) &= -bv, \end{aligned} \quad (14)$$

thus completely defining our initial-value problem. Without loss of generality we may take the values of these parameters according to numerical convenience. Let us set

$$\lambda = 1, \quad a = (2.015, 2.015), \quad b = 1$$

throughout. As depicted in figure 1, the total energy density corresponding to our soliton field has the form of two lumps sitting on the central cross of the cell, symmetrically around its centre.

Consider the situation where the lumps are sent towards one another with a relative initial speed of $v = 0.3$. We observe that the solitons gradually expand as they approach each other; they collide at the centre of the net and coalesce into a ringish structure, where the solitons are no longer distinguishable. Here they attain maximum expansion, *i.e.*, the peak of the total energy density (E_{max}) reaches a minimum value. After this process the lumps get narrower and narrower as they re-emerge at right angles to their initial line of approach. They keep shrinking while moving away from the centre, in opposite senses. Some time later they become so spiky that the numerical code breaks down. This is the well-documented instability of the $O(3)$ model in two dimensions, where the theory is conformally invariant. The foregoing events are illustrated in figure 2.

The evolution of E_{max} is shown in the upper half of figure 3 for two values of v . The curves are qualitatively alike, the life of the system being longer the smaller its initial velocity is.

The kinetic energy remains very small all along except when the instability takes over. This can be appreciated from figure 3 (bottom), where the maximum value of the kinetic energy density (K_{max}) is plotted *versus* time.

Solitons with no initial velocity remain motionless with the passing of time (see below, however, the particular case when $b = 0$). They too exhibit shrinking and singularity formation, if at a slower rate than when $v \neq 0$; the evolution of the total energy density qualitatively resembles that of figure 3 (top). As for the kinetic energy density, it stays very small, at around $\approx 10^{-7}$ during the whole simulation (except when the breadth of the lumps is comparable to the lattice spacing which leads to the collapse of the numerics).

Particularly noteworthy is the case $b = 0$. The soliton field and its energy distribution are, respectively from equations (3) and (10),

$$\begin{aligned} W &= \lambda \wp(z - a), \\ E &= 8|\lambda|^2 \frac{|\wp(z-a)||\wp^2(z-a) - \wp^2(L/2)|}{[1 + |\lambda \wp(z-a)|^2]^2}. \end{aligned} \quad (15)$$

The global maxima of such energy density are located along the diagonals of the basic cell [8], *i.e.*, where $\wp(z)$ is purely imaginary. Given that E in (15) is invariant under $\wp \rightarrow -\wp$, it follows from the evenness of \wp that E has at least for peaks on the diagonals of the fundamental cell. In fact, it possesses four peaks (see figure 4). This situation in the topological index-two class is a remarkable feature of \wp -solitons, going beyond the two-lump and annular structures found in the CP^1 on S_2 .

Now, the scattering problem when $b = 0$ is especial: In order to zoom the lumps towards each other one must boost W according to equation (14), *i.e.*, set $b \rightarrow b(1 - vt)$. But this is only possible if $b \neq 0$. And boosting the parameter a in W is of no avail, for it simply shifts the system as a whole. Let us then consider systems of the form (15) started off from rest. It turns out that such configurations shrink quite slowly with time, as illustrated in the upper graph of figure 5.

From the bottom-right plot of figure 5 we observe that the solitons move away from the centre and back in along the diagonals of the grid in breather-like fashion. The kinetic waves emitted in the process evolve according to the bottom-left side of illustration number 5.

Given similar set-ups, CP^1 lumps with periodic boundary conditions will usually shrink at a slower rate than their relatives with standard boundary conditions. This is because solitons in compact domains as T_2 always coalesce somehow, and these are configurations with E_{max} smaller than when the solitons do not overlap – a situation achievable to a good approximation in non-compact spaces like the extended plane. States with $b = 0$, which correspond to coincident structures that spread themselves all over the cell (see picture 4), have a small E_{max} which evolves quasi-stably as depicted in figure 5. Note that other than through the parameter b , we can always bring the solitons to greater overlapping either by increasing the lump size (λ) or by reducing the torus size (L). This is be useful if we want to run a collision experiment with the same value of b but different initial values of E_{max} .

We point out that in reference [7] our configurations for $b = 0$ exhibited scattering in the Skyrme version of the model, even though the initial speed was zero. We define our Skyrme model on the torus by [compare with the lagrangian (1)]

$$\mathcal{L} = \frac{|\partial_t W|^2 - 2|\partial_z W|^2 - 2|\partial_{\bar{z}} W|^2}{(1 + |W|^2)^2} + \theta_1 \frac{|\partial_z W|^2}{(1 + |W|^2)^4} (|\partial_t W|^2 - |\partial_z W|^2). \quad (16)$$

In this scheme the four energy peaks move and collide along the diagonals and scatter at right angles. Let us emphasise that the extra term in the lagrangian (16) stabilises the CP^1 lumps, *i.e.*, prevents the formation of singularities.

As pointed out in the introduction, our main results for \wp -solitons (singularity formation and scattering at 90°) conform with prognostications made in the geodesic approximation treatment of the model [8]. There it was proved that the moduli space of static 2-lump solutions is geodesically incomplete and has finite diameter, leading to infinite lump shrinkage. It was also proved in [8] that some mathematical constraints oblige the lumps to lie either on the central cross, the boundary or the diagonals of the lattice, implying that only scattering at right angles should occur.

5 Conclusions

With the help of numerical simulations we have investigated some scattering properties of the (2+1) dimensional nonlinear $O(3)$ or CP^1 model with periodic boundary conditions, expressing the soliton solutions through Weierstrass' elliptic \wp -function. Limiting ourselves to the pure version of the model, we have observed that the lumps scatter off forming 90° with the initial direction of motion in the centre-of-mass frame. During this process the lumps grow spiker as time elapses, eventually breaking down the numerical code. Lack of stability shows as well for lumps with zero initial speed, but at a slower rate. The $O(3)$ instability may be understood from the symmetry of the model under dilation transformations. The above properties are basically the same as those known from the familiar model on the Riemann sphere. But some other phenomena turn out to be quite disimilar on T_2 , *e.g.*, the absence of unit-charge solitons and the presence of four lumps rather than two in the charge-two topological class. The non-existence of single-soliton fields on T_2 is dictated by a general property stating that there are no elliptic functions of order one. The four peaks in the charge-two sector stem from a notable symmetry property specific to the \wp -energy density when $b = 0$ [see equation (15)]. A configuration of this type is not observed when the fields are constructed out of the σ -function.

A natural extension of the present work is the study of \wp -lumps with non-zero initial velocity in the Skyrme format. Skyrmions with such initial conditions have already shown a thought-provoking scattering and splitting pattern under numerical simulations. Consequently, research

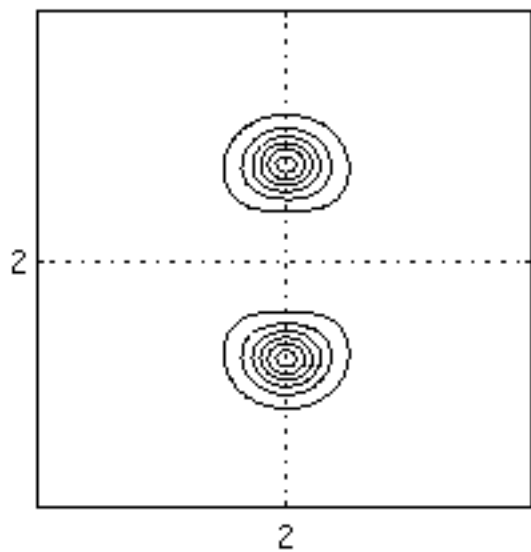
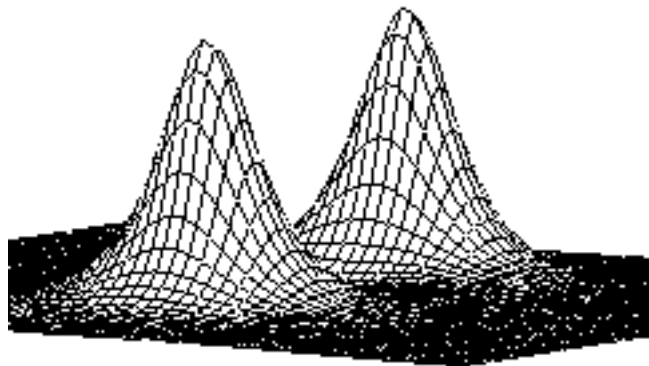
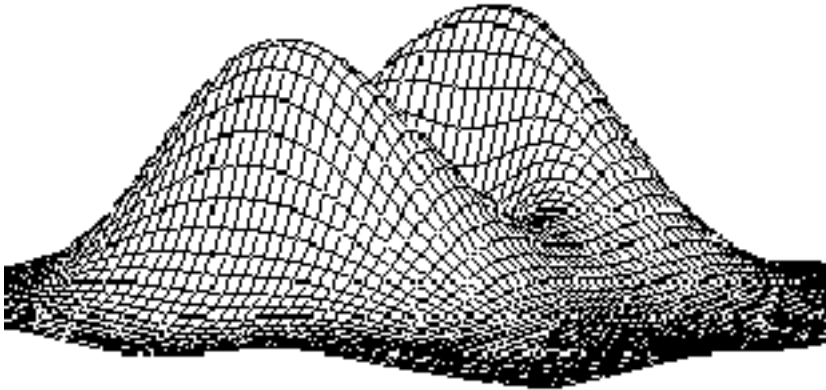


Figure 1: Three dimensional and contour pictures corresponding to the total energy density of the solitons at $t = 0$. The initial speed is $v = 0.3$.

$E_{\max}=16.4; t=3$



$E_{\max}=10.6; t=4.5$

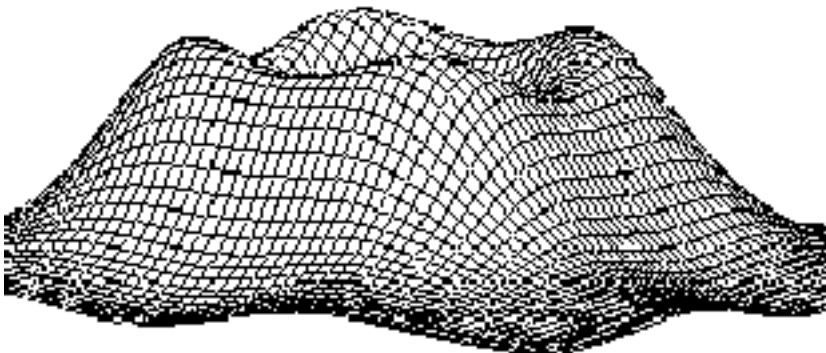
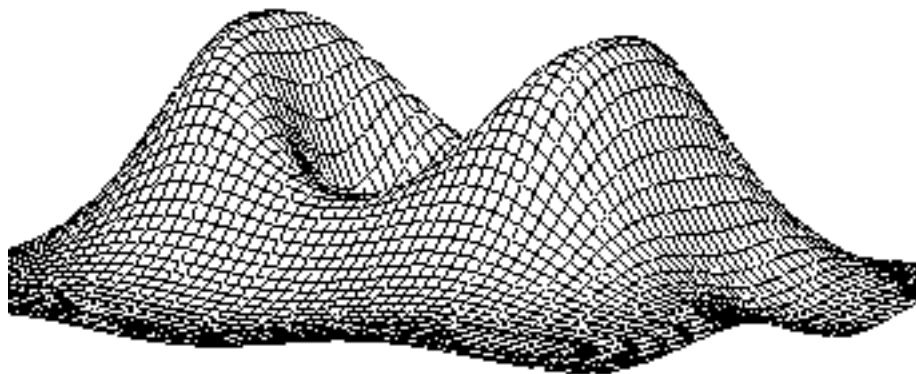


Figure 2: The lumps of figure 1 motion towards each other. They collide and coalesce around the centre of the lattice, where they expand maximally.

$E_{\max}=12.8; t=6$



$E_{\max}=64.5; t=10$

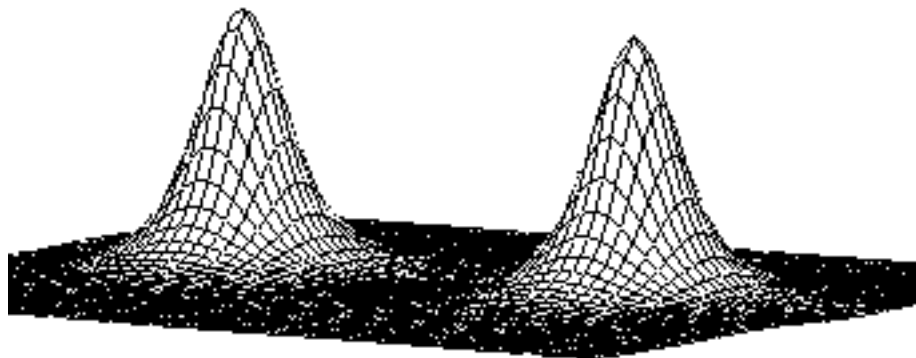


Figure 2: Continued. The lumps scatter at 90° to the original direction of motion.

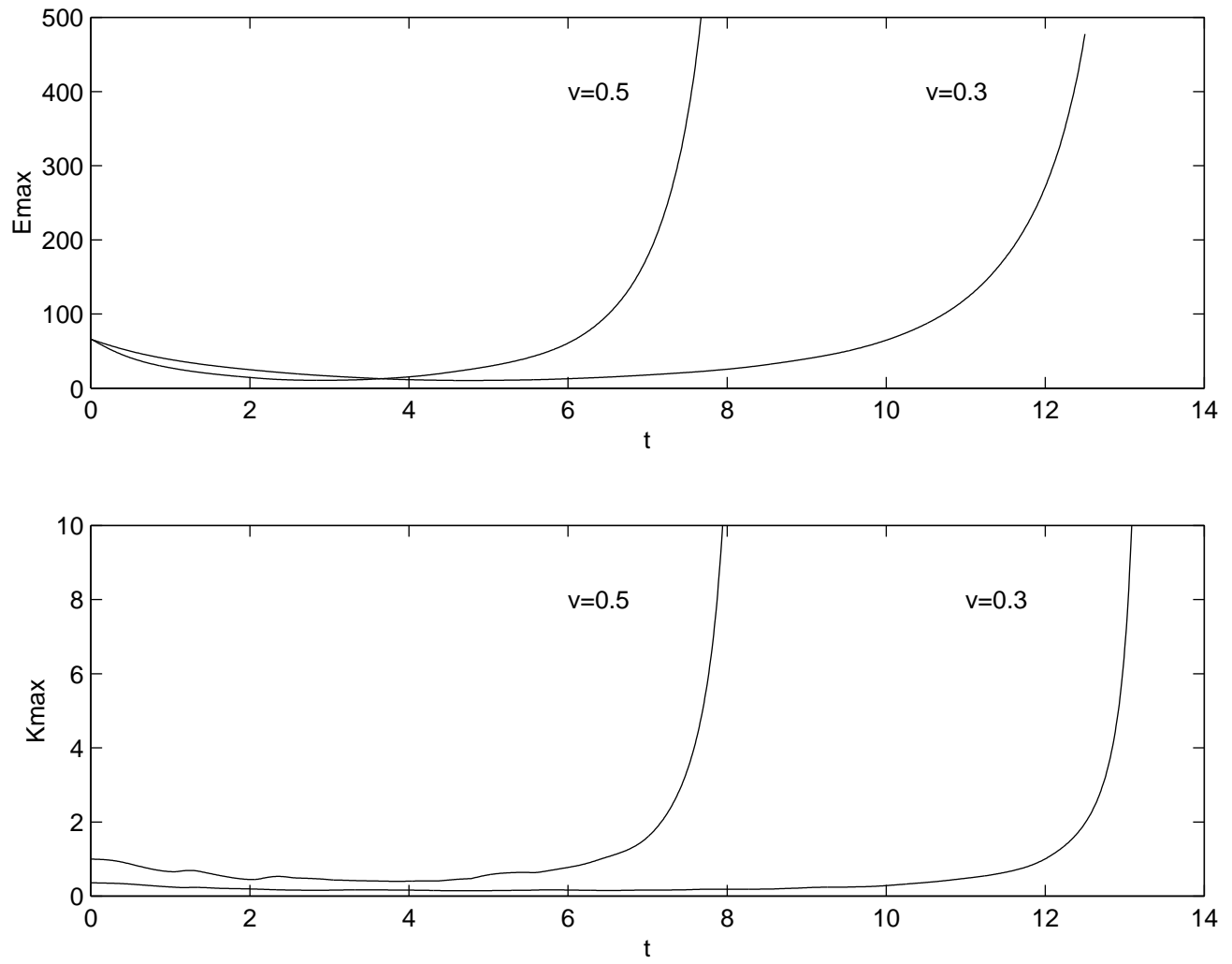


Figure 3: Evolution of the peak of the total energy density (E_{max}) and the peak of the kinetic energy density (K_{max}) for two values of the initial speed.

Lumps at the initial time for the case $b=0$

$E_{\max}=10.94$

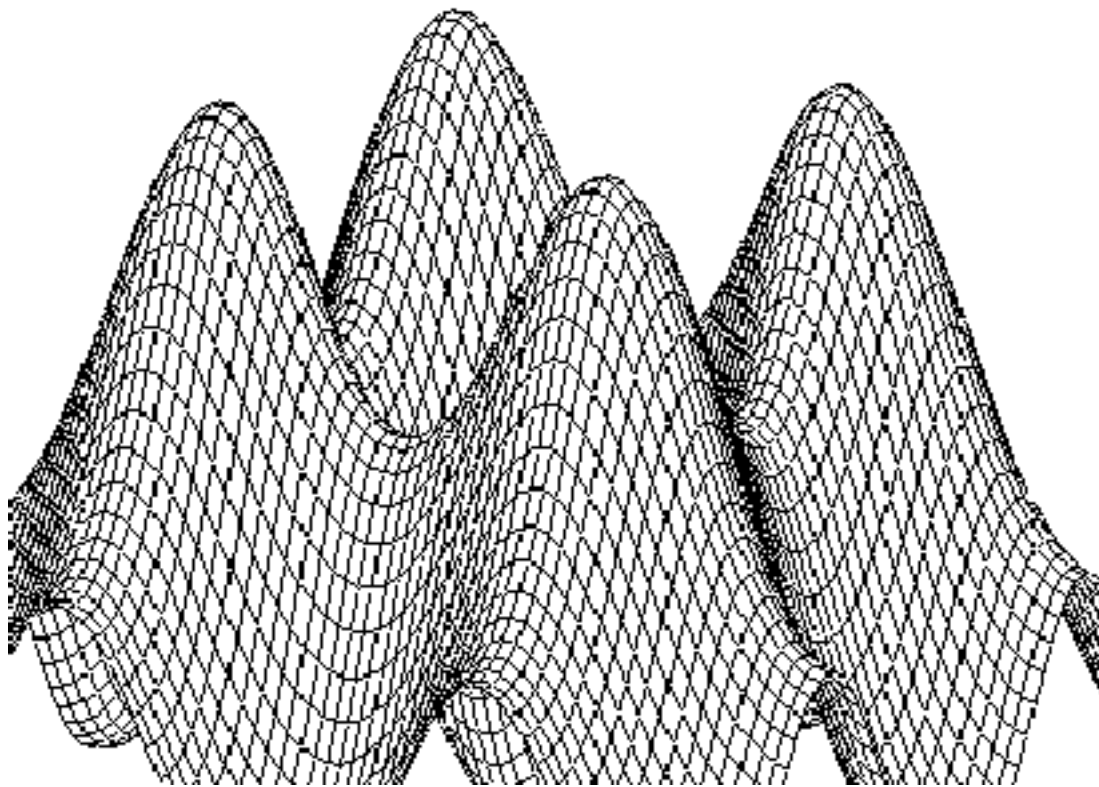


Figure 4: Lumps at $t = 0$ corresponding to the particular case $W = \varphi(z - a)$. The presence of four lumps rather than two in the charge two sector is an alluring characteristic of φ -solitons.

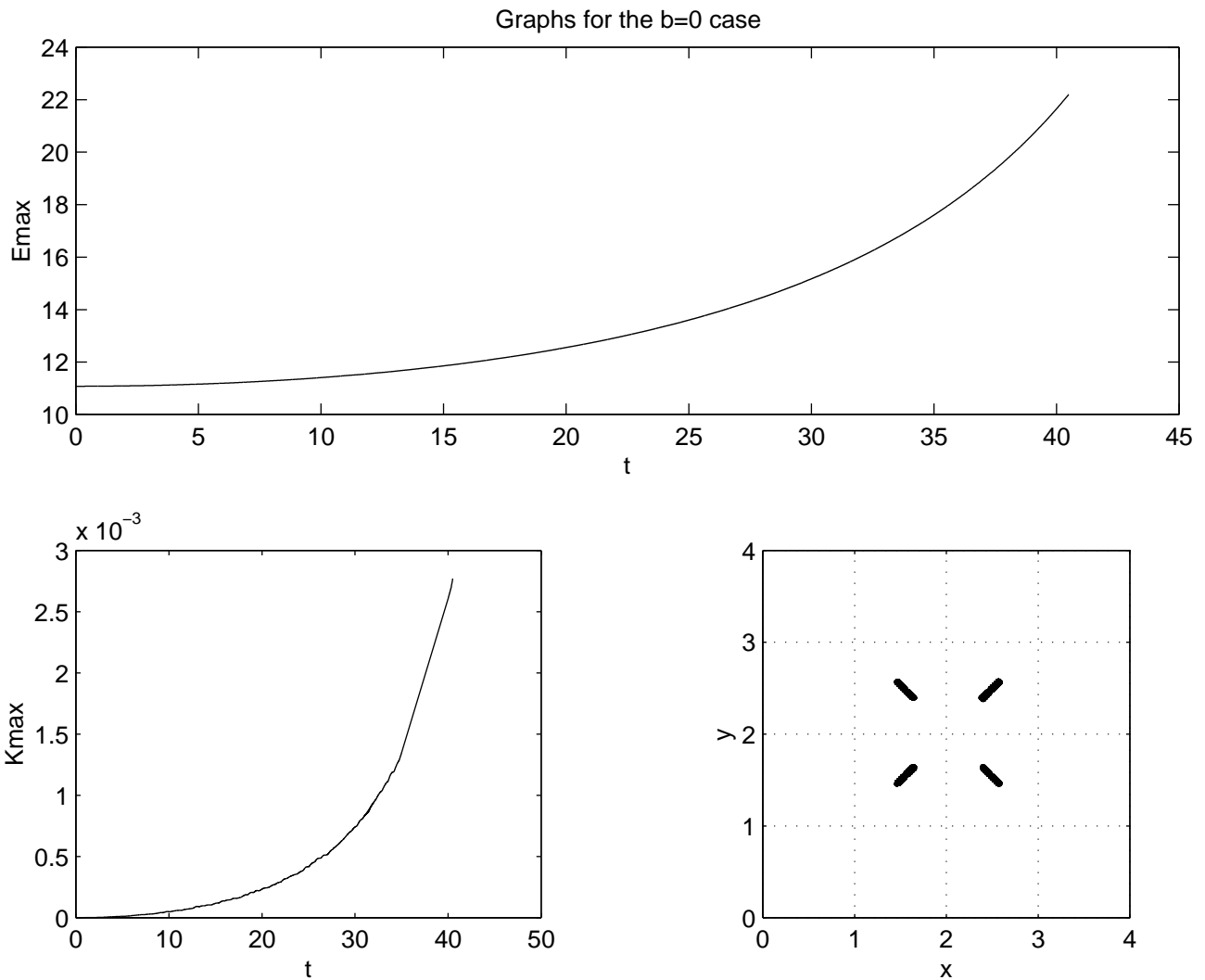


Figure 5: Plots corresponding to $W = \wp(z - a)$. We observe a quasi-stable configuration where the lumps oscillate along the diagonals of the network in breather-like manner. The initial velocity is zero.

on their evolution under boosting seems compelling. Further investigations may involve defining the solitons in terms of other elliptic functions as those of Jacobi, and the pseudo-elliptic θ -functions. A classification of solitonic properties on the torus can only be made after thorough consideration of the above-mentioned functions. Let us remind that on S_2 no new traits arise from casting the soliton configurations in different ways. In the topological charge two class, for example, the following fields behave qualitatively alike on the Riemann sphere:

$$W = z^2, z^{-2}, \frac{(z-a)(z-b)}{(z-c)(z-d)}.$$

It is a non-trivial problem to understand the mechanisms underlying the complicated CP^1 dynamics. In the quest for such understanding, a study of solitonic behaviour on compact manifolds, especially T_2 , is certainly quite an appealing program to pursue.

Acknowledgement

The author is very grateful to WJ Zakrzewski for helpful conversations and to the Mathematical Sciences Dept. of the University of Durham, England, where part of the present work was carried out. The financial support of *La Universidad del Zulia* through CONDES 218-99 is acknowledged with big thanks.

References

- [1] Eichenherr H. (1976) Nucl. Phys. **B146**, 215
- [2] Perelomov A. M. (1981) Physica **4D**, (1981) 1
- [3] Zakrzewski W. J. (1991) Nonlinearity **4**, 429
- [4] Leese R. A., Peyrard M. and Zakrzewski W. J. (1990) Nonlinearity **3**, 387
- [5] Cova R. J. (1995) Helv. Phys. Acta **8**, 282
- [6] Cova R. J. and Zakrzewski W. J. (1997) Nonlinearity **10**, 1305
- [7] Cova R. J. (1998) Helv. Phys. Acta **71**, 675
- [8] Speight J. M. (1998) Comm. Math. Phys **194**, 513
- [9] Goursat E. (1916) Functions of a complex variable, Dover Publications
- [10] Lawden D. F. (1989) Elliptic functions and applications, Springer Verlag USA